The Astrophysical Journal Letters, 956:L39 (4pp), 2023 October 20 https://doi.org/10.3847/2041-8213/acfe6e
© 2023. The Author(s). Published by the American Astronomical Society.
OPEN ACCESS

PSR J1953+1844 Probably Being the Descendant of an Ultracompact X-Ray Binary

Z. L. Yang[1,2,3], J. L. Han[1,2,3], W. C. Jing[1,2,3], and W. Q. Su[1,2,3]
[1] National Astronomical Observatories, Chinese Academy of Sciences, Beijing 100101, People's Republic of China; hjl@bao.ac.cn
[2] School of Astronomy and Space Sciences, University of Chinese Academy of Sciences, Beijing 100049, People's Republic of China
[3] CAS Key laboratory of FAST, National Astronomical Observatories, Chinese Academy of Sciences, Beijing 100101, People's Republic of China
Received 2023 June 29; revised 2023 September 2; accepted 2023 September 28; published 2023 October 18

Abstract

PSR J1953+1844 (i.e., M71E) is a millisecond pulsar in a 53 minute binary orbit discovered by the Five-hundred-meter Aperture Spherical radio Telescope. The mass function from pulsar timing is $2.3 \times 10^{-7}\ M_{\odot}$. The possible redback origin of this system has been discussed by Pan et al. We discuss here an alternative evolution track for this binary system, namely that PSR J1953+1844 is a descendant of an ultracompact X-ray binary (UCXB), which has a hydrogen-poor donor accreting onto a neutron star (NS) with an orbital period of $\leqslant$1 hr. We noticed that some UCXB systems hold an accreting millisecond X-ray pulsar (AMXP) and a donor with a mass of about 0.01 $M_{\odot}$. M71E has a very similar orbit to those of AMXPs, indicating that it might be evolved from a UCXB similar to PSR J1653–0158. The companion star of M71E should be significantly bloated and it most probably has a carbon and oxygen composition, otherwise a low inclination angle of the orbit is required for a helium companion. The discovery of this M71E binary system may shed light on when and how an NS in a UCXB turns into a radio pulsar.

Unified Astronomy Thesaurus concepts: Binary pulsars (153); X-ray binary stars (1811); Low-mass x-ray binary stars (939); Compact binary stars (283)

1. Introduction

Soon after the discovery of a radio millisecond pulsar (MSP; Backer et al. 1982), it was suggested that such a fast-rotating object may be originated from an ultracompact X-ray binary (UCXB). Nowadays a large number of accreting MSPs have been found in UCXBs (Wijnands 2010; Strohmayer et al. 2018; Ng et al. 2021). However, the transition from accretion-powered MSPs in UCXBs to these rotation-powered pulsars is not yet well understood (Heinke et al. 2013). Traditionally, eclipsing MSPs in a tight orbit (orbital period $P_{\rm orb} \leqslant 1$ day) with a companion of mass 0.1–0.4 $M_{\odot}$ are classified as redbacks, while those MSPs orbiting a companion of mass $\ll$0.1 $M_{\odot}$ are classified as black widows (Chen et al. 2013; Roberts 2013). The two systems are the subclasses of spider pulsars whose companion stars are suffering from severe mass loss. Among them, black widows with an orbital period less than 2 hr, e.g., PSR J1653−0158 (Nieder et al. 2020), PSR J1719−1438 (Bailes et al. 2011), and PSR J0636+5128 (Kaplan et al. 2018), are believed to be the descendants of UCXBs. It was proposed that the pulsar wind may play an important role in this transition process, and binary pulsars will form from UCXBs with an orbital period of ∼1.5 hr (Bailes et al. 2011; Heinke et al. 2013).

Recently a binary pulsar PSR J1953+1844 (i.e., M71E, because it is probably located in the globular cluster M71) was discovered by the Five-hundred-meter Aperture Spherical radio Telescope (FAST; Nan 2006; Nan et al. 2011) during the FAST Galactic Plane Pulsar Snapshot (GPPS) survey (Han et al. 2021). The follow-up timing observations have revealed that M71E has an orbit period of 53 minutes (Pan et al. 2023). Its short orbit period of 53 minutes breaks the previous record for the orbit period of 75 minutes for PSR J1653–0158 (Nieder et al. 2020); no eclipses and significant orbital period changes have been detected yet (Pan et al. 2023). The nature of this system is not well understood yet. This system was interpreted as an intermediate between redbacks and black widows by Pan et al. (2023). Based on a low mass function of $2.3 \times 10^{-7}\ M_{\odot}$ and the strikingly short orbital period in the range of UCXB orbital periods, here we discuss an alternative evolution scenario for this binary system, namely that it is a newly evolved descendant of a UCXB, as a complementary theory to Pan et al. (2023). We discuss in this Letter the evolution and fate of this binary system, and suggest that the companion of M71E is a hydrogen-poor star with a mass of ∼0.01 $M_{\odot}$.

2. FAST Results and Binary Constraints

M71E has a spin period of 4.44 ms (Han et al. 2021). It has been suspected to be not physically associated with the globular cluster (Pan et al. 2021) though its dispersion measure (DM) is very close to the DMs of known pulsars inside the cluster. More follow-up observations by the FAST over 1.5 yr yield an excellent phase-link timing solution, including the derivative of pulsar spin period ($1.1 \times 10^{-15}\ {\rm s}^{-2}$) and exact position. At the outskirt of M71 at a distance of 4 kpc, the kinetics contribution on the spin frequency derivative from the global cluster is at most $2 \times 10^{-16}\ {\rm s}^{-2}$ (Baumgardt & Hilker 2018), roughly 1 order smaller than the measured value. We therefore trust that a spin-down luminosity of $\dot{E} = I\Omega\dot{\Omega} = 1 \times 10^{34}\ {\rm erg\ s}^{-1}$ is reliable, a typical value for spider pulsars.

The mass function from the timing solution of M71E is $2.3 \times 10^{-7}\ M_{\odot}$ (Pan et al. 2023), which is related to the companion mass, pulsar mass, and orbital inclination by

$$f(m) = (M_{\rm c} \sin i)^3 / (M_{\rm NS} + M_{\rm c})^2. \quad (1)$$

Using the recycled-pulsar mass distribution from Özel & Freire (2016) and a random orbital orientation, we get that its companion mass is in the range of 8–15 $\times 10^{-3}\ M_{\odot}$ at the 68%

Original content from this work may be used under the terms of the Creative Commons Attribution 4.0 licence. Any further distribution of this work must maintain attribution to the author(s) and the title of the work, journal citation and DOI.

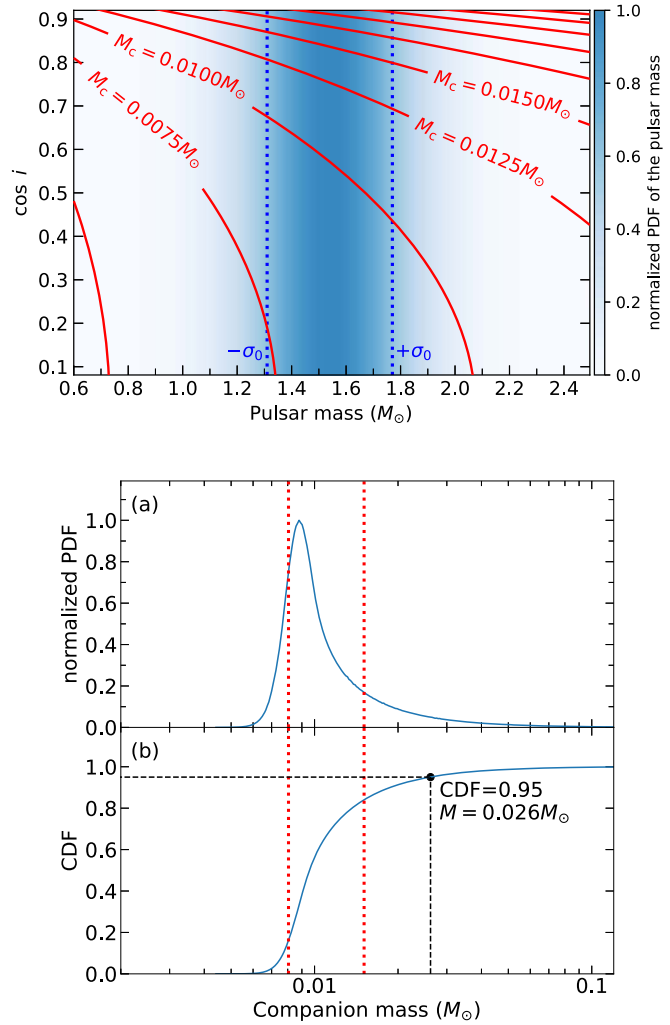


Figure 1. The probability distribution of the companion mass M_c of M71E. Top panel: distribution of possible companion mass calculated for various inclination angle i and pulsar mass M_{psr}. Here, $\cos i$ should follow a uniform probability distribution if the orbital orientation is random in space. The probability density function (pdf) for the pulsar mass presented in the gray scale is taken from Özel & Freire (2016) for the recycled pulsars, following a Gaussian function centering at $M_0 = 1.54\,M_\odot$ with a standard deviation of $\pm\sigma_0 = 0.23\,M_\odot$ as indicated by two dotted lines. Bottom panel: the pdf (in subpanel (a)) and the cumulative distribution function (CDF, in subpanel (b)) for the companion mass M_c integrated from the pdf on the top panel, with a probability of $\cos i$ uniformly distributed in the range of (0, 1). Two red dotted lines indicate the companion mass of 0.008 and 0.015 $M_\odot$ at the 16% and 84% probability ($\pm1\sigma$) of the CDF and the dashed line marked the 95% probability of the CDF at 0.026 $M_\odot$.

confidence level ($\pm1\sigma$) and $<0.026\,M_\odot$ at the 95% confidence level, as shown in Figure 1. The short orbital period of M71E and a flyweight companion of mass $\sim0.01\,M_\odot$ bear a striking resemblance to many UCXBs (see Figure 2).

At the accurate timing position of pulsar, a faint X-ray source (Pan et al. 2023) and an optical counterpart (Liu & Dong 2023) are found. The X-ray counterpart that we identified for this system is 2CXO J195337.9+184454 from Evans et al. (2010), which has a X-ray luminosity of 1×10^{30} erg s^{-1} in 0.5−7.0 keV, about 10^{-4} of M71E's spin-down luminosity. We noticed that Zhao & Heinke (2023) also identified this source. They fitted a blackbody-like model and got a X-ray luminosity of $1.9^{+1.2}_{-1.1} \times 10^{30}$ erg s^{-1}, similar to those of other noneclipsing black widows (Zhao & Heinke 2023).

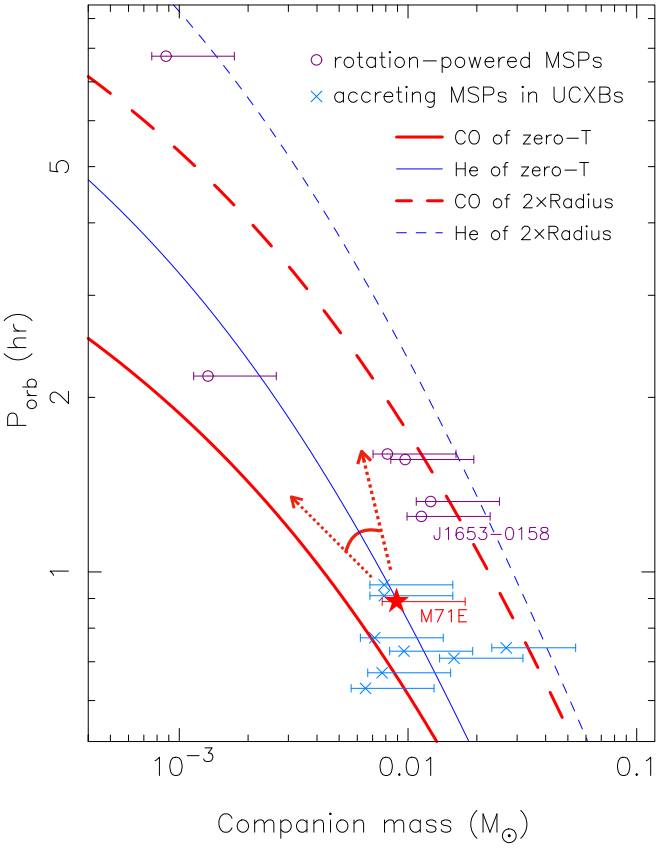


Figure 2. Companion mass vs. orbital period for accreting MSPs in UCXBs and possible rotation-powered pulsar descendants. Data are taken from Guo et al. (2022), ATNF pulsar catalog (Manchester et al. 2005), and also Table 4.1 in Bhattacharyya et al. (2022). The error bars represent the mass range of these systems from $\cos i = 0$ to $\cos i = 0.9$ (90% possibility) assuming a 1.4 $M_\odot$ neutron star mass, with the median companion mass calculated at $\cos i = 0.5$ marked by circles and crosses for rotation-powered MSPs or accretion-powered MSPs, respectively. The binary system with a zero-temperature (zero-T) companion with a filled Roche lobe is indicated by solid curves, while that holds a companion with a zero-T radius of only one-half of the Roche lobe radius is indicated by dashed curves (Paczyński 1971; Rappaport et al. 1987). M71E is marked as a star. The parameter range roughly indicated by the two arrows is the possible long-term evolution direction in the parameter space.

The optical counterpart identified by Liu & Dong (2023) should have a variation if the orbit is not face on, though it has not yet detected. The temperature difference between the heated side (dayside) and the unheated side (nightside) can be estimated base on the spin-down power $\dot{E}$ of the pulsar (Romani & Sanchez 2016),

$$T_D^4 - T_N^4 = \eta \dot{E}/4\pi a^2 \sigma_{SB}, \quad (2)$$

where T_D and T_N are the effective temperatures of the heated side and unheated side respectively, η is the heating efficiency, and a is the orbital separation. The heating efficiency varies from system to system, and in some systems it can be even larger than 1 due to anisotropic emission (Romani & Sanchez 2016). Assuming a Roche lobe filling factor of f, a pulsar mass of 1.4 $M_\odot$ and a companion mass of 0.01 $M_\odot$, we find that the heated side temperature should be about 10^4 K for a heating efficiency about 1, and the equivalent luminosity of the companion star on the heated side is at least $0.02\eta f^2\,L_\odot$, which is very sufficient to explain the luminosity of its optical counterpart with an assumption of blackbody-like radiation

with $E_{10^4k}/E_{4500k}(\lambda = 606\,\mathrm{nm}) = 0.82\ L_{10^4\mathrm{K}}/L_{4500\mathrm{K}}$ (Liu & Dong 2023).

3. Evolution of M71E

Referring to Figure 2, the M71E binary system has an orbital period even shorter than those of some known UCXBs, which makes the formation and evolution picture more complicated. This radio MSP probably was formed from a UCXB at an earlier evolutionary stage in the transition from AMXPs to radio MSPs.

3.1. The Mass Transfer Phase

Depending on different types of donor stars, such as white dwarfs (WDs) or helium stars or main-sequence (MS) stars (Pringle & Webbink 1975; Nelson et al. 1986; Savonije et al. 1986; Podsiadlowski et al. 2002; Yungelson et al. 2002; Yungelson 2008; Sengar et al. 2017; Chen et al. 2022; Guo et al. 2022), the evolution routines of UCXBs are quite different. WD donors become fully degenerate very quickly. However, with the helium star donor and the MS donor, the system should experience a long time of mass transfer from the donor star, and then it is degenerated and thermally relaxed. Afterwards, the evolution tracks for various UCXBs in these scenarios are very similar (van Haaften et al. 2012b). In a stable mass transfer phase, the donor star has a radius R_c roughly equal to its Roche lobe radius R_L. Given the well-known mass–radius relationship for the degenerated star $R \propto M^{\beta}$ ($\beta = -1/3$), the donor stars should expand in response to the mass loss (Deloye & Bildsten 2003; van Haaften et al. 2012b; Heinke et al. 2013). As a result, their orbital periods increase to keep $R_c \approx R_L$.

3.2. The Roche Lobe Detachment Phase

With a circular orbit, the orbital angular momentum of a UCXB for a neutron star (NS) accretor can be written as

$$J_{\mathrm{orb}}^2 = \frac{GM_c^2M_{\mathrm{Nd}}^2}{M_{\mathrm{tot}}}a, \tag{3}$$

where J_{orb} is the orbital angular momentum, a is the orbital separation, M_c is the companion mass, and M_{Nd} is the sum of the NS mass M_{NS} and the accretion disk mass M_{disk} in the vicinity of the NS. The combination of this equation and the Kepler's third law leads to

$$2\frac{\dot{J}_{\mathrm{orb}}}{J_{\mathrm{orb}}} = 2\left(\frac{\dot{M}_c}{M_c} + \frac{\dot{M}_{\mathrm{Nd}}}{M_{\mathrm{Nd}}}\right) - \frac{\dot{M}_{\mathrm{tot}}}{M_{\mathrm{tot}}} + \frac{\dot{a}}{a} \tag{4}$$

and

$$3\frac{\dot{a}}{a} - 2\frac{\dot{P}_{\mathrm{orb}}}{P_{\mathrm{orb}}} = \frac{\dot{M}_{\mathrm{tot}}}{M_{\mathrm{tot}}}. \tag{5}$$

In the detachment phase, we take $R_c = R_L$ and $\dot{R}_c < \dot{R}_L$. Given that $R_c \propto M_c^{\beta}$ and in the case $M_c \ll M_{\mathrm{Nd}}$, one gets $R_L \propto a(M_c/M_{\mathrm{Nd}})^{1/3}$ (Paczyński 1971; Eggleton 1983). That is to say

$$\beta\frac{\dot{M}_c}{M_c} < \frac{1}{3}\left(\frac{\dot{M}_c}{M_c} - \frac{\dot{M}_{\mathrm{Nd}}}{M_{\mathrm{Nd}}}\right) + \frac{\dot{a}}{a}. \tag{6}$$

With a flyweight donor, the orbital angular momentum loss is dominated by mass loss. Similar to van den Heuvel (1994) and Soberman et al. (1997), one can get

$$\delta J_{\mathrm{orb}} = \delta M_1\frac{M_{\mathrm{Nd}}}{M_cM_{\mathrm{tot}}}J_{\mathrm{orb}} + \delta M_2\frac{M_c}{M_{\mathrm{Nd}}M_{\mathrm{tot}}}J_{\mathrm{orb}}, \tag{7}$$

where δM_1 is the mass lost from the donor star as fast isotropic winds, and δM_2 is the mass ejected from the vicinity of the NS in an isotropic way. At the time of detachment, there is no Roche lobe overflow, therefore the main mass loss is the evaporation of the companion caused by the pulsar wind. This leads to $\delta M_1 = \delta M_c$ and $\delta M_2 = \delta M_{\mathrm{Nd}} = 0$. Combining them with Equation (4), one can obtain $\dot{a}/a = -\dot{M}_c/M_{\mathrm{tot}}$. Then in Equation (7), one gets $\beta > \frac{1}{3}$.

For degenerated stars the mass–radius relationship requires $\beta < 0$ until the mass of object is below the maximum-radius mass value (Rappaport et al. 1987), which should not be the case for the companion mass of M71E. The donor star should have a nondegenerate outer layer so that the detachment scenario becomes possible. The shrinkage of the companion radius may be not driven by mass loss, but could be a decrease in the heating by the pulsar or a more efficient cooling (van Haaften et al. 2012a). Such a bloated companion is also supported by a high temperature derived from Equation (2) and optical observations of similar systems (Kandel & Romani 2023), and this system may experience cycles of expansion and shrinkage as suggested by Ritter et al. (2000). In Figure 2, an bloated companion should be in the very right side of the zero-temperature (zero-T) line in Figure 2. However, M71E is located by chance on the He zero-T line in Figure 2, and on the very right side of the CO zero-T line; therefore a CO WD is more likely for any inclination angles of the orbit. If it is a He WD, a very low inclination angle is strongly desired, which is much less likely to exist.

Another possible mechanism for the detachment of M71E's companion involves the disk instability (van Haaften et al. 2012a; Guo et al. 2022). A stable helium-composition disk requires the lowest mass transfer rate (Lasota 2001; Menou et al. 2002; in't Zand et al. 2007; van Haaften et al. 2012b)

$$\dot{M}_{\mathrm{crit}} \approx 3 \times 10^{-10}\left(\frac{M_c}{M_\odot}\right)^{0.3}\left(\frac{P_{\mathrm{orb}}}{\mathrm{hr}}\right)^{1.4} M_\odot\ \mathrm{yr}^{-1}, \tag{8}$$

below which a thermal-viscous instability appears and the disk experiences outbursts. The outburst causes a sudden decrease of the disk mass; therefore $\delta M_1 = \delta M_c = 0$ and $\delta M_2 = \delta M_{\mathrm{Nd}} \geqslant -M_{\mathrm{disk}}$. The material is ejected from the vicinity of the NS, taking away its orbital angular momentum (Wang et al. 2021). Again using Equation (4), we obtain $\delta a = a(-\delta M_2/M_{\mathrm{tot}})$, which leads to a sudden increase of the Roche lobe radius without changes in companion size. The companion becomes detached. This detachment scenario may lead to a similar behavior of transitional MSPs (Archibald et al. 2009), which switch back and forth between the X-ray and radio pulsar state (van Haaften et al. 2012a).

3.3. Roche Lobe Reattachment

The companion radius should be in the range between its zero-T radius and Roche lobe radius, providing a constraint of its density $\rho_{c,\mathrm{zero}-T} > \rho_c > \rho_{c,R_c=R_L}$.

After the Roche lobe detachment, the long-term evolution is dominated by the evaporation of the companion caused by the

pulsar wind. The companion mass is lost by fast isotropic winds, and the lost mass also carries away the orbital angular momentum. Using Equations (4), (5), and (7), we obtain $\dot{P}_{\rm orb}/P_{\rm orb} = -2\dot{M}_{\rm c}/M_{\rm tot}$, the same as Jeans (1924). This has been widely taken as the contribution from the companion mass loss on the variations of the orbital period in spider pulsar systems (Lazaridis et al. 2011; Pletsch & Clark 2015; Kumari et al. 2023). When this mass-loss effect dominates the variations of orbital period, one gets $P_{\rm orb} \propto M_{\rm tot}^{-2}$. The changes in total mass of this system are relatively small, so the orbital period nearly freezes while the companion mass continues to decrease. Before the system crosses the solid curves (reaching $\rho_{\rm c,zero-}{}_T \leqslant \rho_{\rm c,}{}_{R_{\rm c}=R_{\rm L}}$), a reattachment of M71E's companion is inevitable. If the companion star has a size close to its Roche lobe, the Roche lobe reattachment may not be driven by mass loss and may happen much more quickly as a part of cyclic behaviors (Ritter et al. 2000; van Haaften et al. 2012a). After that, a new Roche lobe overflow phase begins, during which its orbital period will increase to keep $R_{\rm c} \approx R_{\rm L}$ as discussed in Section 3.1. As shown roughly by the two red arrows in Figure 2, the system will evolve toward the upper left corner in this parameter space, and becomes a system similar to other descendants of UCXBs, such as PSR J1653–0158 (Nieder et al. 2020).

4. Conclusion

Discovered during the FAST GPPS survey (Han et al. 2021), M71E is a remarkable binary pulsar due to the shortest orbital period among all known rotation-powered pulsar binaries (Pan et al. 2023). According to the mass function, the companion mass of M71E is $\sim 0.01\,M_{\odot}$, and the orbit of this system is strikingly similar to that of AMXPs in ultracompact X-ray binaries (see Figure 2). Therefore a probable alternative explanation is that M71E is a descendant from a UCXB. This was briefly mentioned in Pan et al. (2023) and now discussed in detail here as a complementary theory.

In this scenario, M71E has a very short orbital period so it is in a much earlier evolutionary stage compared to other radio MSPs that are descendants of UCXBs. The possible evolution of M71E is that a natural detachment from the Roche lobe happens when $\beta > \frac{1}{3}$, which means that the companion density increases with the mass loss. A nondegenerate outer layer is required in this scenario, and it favors a CO-rich companion. If it is a He WD, a low inclination angle of the orbit is strongly desired, which is much less likely to exist. Another possibility involves X-ray outbursts caused by the disk instability, and we then expect M71E to behave like a transitional MSP. In both cases, a reattachment of M71E's companion is inevitable in the future. We suggest that in the late evolution stage, the MSPs in UCXBs will experience several transitions between a radio pulsar and an accretion-powered X-ray pulsar.

Acknowledgments

The authors are supported by the Natural Science Foundation of China, Nos. 11988101, 11833009, and also the National SKA Program of China, No. 2022SKA0120103. We thank Dr. YunLang Guo and Prof. HaiLiang Chen for helpful comments.

ORCID iDs

Z. L. Yang https://orcid.org/0009-0009-6590-1540
J. L. Han https://orcid.org/0000-0002-9274-3092
W. C. Jing https://orcid.org/0000-0002-1056-5895
W. Q. Su https://orcid.org/0009-0003-2212-4792

References

Archibald, A. M., Stairs, I. H., Ransom, S. M., et al. 2009, Sci, 324, 1411
Backer, D. C., Kulkarni, S. R., Heiles, C., Davis, M. M., & Goss, W. M. 1982, Natur, 300, 615
Bailes, M., Bates, S. D., Bhalerao, V., et al. 2011, Sci, 333, 1717
Baumgardt, H., & Hilker, M. 2018, MNRAS, 478, 1520
Bhattacharyya, S., Papitto, A., & Bhattacharya, D. 2022, in Astrophysics and Space Science Library, Millisecond Pulsars, ed. S. Bhattacharyya, A. Papitto, & D. Bhattacharya, Vol. 465 (Cham: Springer), 319
Chen, H.-L., Chen, X., Tauris, T. M., & Han, Z. 2013, ApJ, 775, 27
Chen, H.-L., Tauris, T. M., Chen, X., & Han, Z. 2022, ApJ, 930, 134
Deloye, C. J., & Bildsten, L. 2003, ApJ, 598, 1217
Eggleton, P. P. 1983, ApJ, 268, 368
Evans, I. N., Primini, F. A., Glotfelty, K. J., et al. 2010, ApJS, 189, 37
Guo, Y., Wang, B., & Han, Z. 2022, MNRAS, 515, 2725
Han, J. L., Wang, C., Wang, P. F., et al. 2021, RAA, 21, 107
Heinke, C. O., Ivanova, N., Engel, M. C., et al. 2013, ApJ, 768, 184
in't Zand, J. J. M., Jonker, P. G., & Markwardt, C. B. 2007, A&A, 465, 953
Jeans, J. H. 1924, MNRAS, 85, 2
Kandel, D., & Romani, R. W. 2023, ApJ, 942, 6
Kaplan, D. L., Stovall, K., van Kerkwijk, M. H., Fremling, C., & Istrate, A. G. 2018, ApJ, 864, 15
Kumari, S., Bhattacharyya, B., Kansabanik, D., & Roy, J. 2023, ApJ, 942, 87
Lasota, J.-P. 2001, NewAR, 45, 449
Lazaridis, K., Verbiest, J. P. W., Tauris, T. M., et al. 2011, MNRAS, 414, 3134
Liu, Z., & Dong, S. 2023, ApJ, 956, 33
Manchester, R. N., Hobbs, G. B., Teoh, A., & Hobbs, M. 2005, AJ, 129, 1993
Menou, K., Perna, R., & Hernquist, L. 2002, ApJL, 564, L81
Nan, R. 2006, ScChG, 49, 129
Nan, R., Li, D., Jin, C., et al. 2011, IJMPD, 20, 989
Nelson, L. A., Rappaport, S. A., & Joss, P. C. 1986, ApJ, 304, 231
Nieder, L., Clark, C. J., Kandel, D., et al. 2020, ApJ, 902, L46
Ng, M., Ray, P. S., Bult, P., et al. 2021, ApJL, 908, L15
Özel, F., & Freire, P. 2016, ARA&A, 54, 401
Paczyński, B. 1971, ARA&A, 9, 183
Pan, Z., Lu, J. G., Jiang, P., et al. 2023, Natur, 620, 961
Pan, Z., Qian, L., Ma, X., et al. 2021, ApJL, 915, L28
Pletsch, H. J., & Clark, C. J. 2015, ApJ, 807, 18
Podsiadlowski, P., Rappaport, S., & Pfahl, E. D. 2002, ApJ, 565, 1107
Pringle, J. E., & Webbink, R. F. 1975, MNRAS, 172, 493
Rappaport, S., Nelson, L. A., Ma, C. P., & Joss, P. C. 1987, ApJ, 322, 842
Ritter, H., Zhang, Z. Y., & Kolb, U. 2000, A&A, 360, 959
Roberts, M. S. E. 2013, in Proc. of the IAU, Neutron Stars and Pulsars: Challenges and Opportunities after 80 years, ed. J. van Leeuwen, 291 (Cambridge: Cambridge Univ. Press), 127
Romani, R. W., & Sanchez, N. 2016, ApJ, 828, 7
Savonije, G. J., de Kool, M., & van den Heuvel, E. P. J. 1986, A&A, 155, 51
Sengar, R., Tauris, T. M., Langer, N., & Istrate, A. G. 2017, MNRAS, 470, L6
Soberman, G. E., Phinney, E. S., & van den Heuvel, E. P. J. 1997, A&A, 327, 620
Strohmayer, T. E., Arzoumanian, Z., Bogdanov, S., et al. 2018, ApJL, 858, L13
van den Heuvel, E. P. J. 1994, Saas-Fee Advanced Course 22: Interacting Binaries (Berlin: Springer), 263
van Haaften, L. M., Nelemans, G., Voss, R., & Jonker, P. G. 2012a, A&A, 541, A22
van Haaften, L. M., Nelemans, G., Voss, R., Wood, M. A., & Kuijpers, J. 2012b, A&A, 537, A104
Wang, B., Chen, W.-C., Liu, D.-D., et al. 2021, MNRAS, 506, 4654
Wijnands, R. 2010, HiA, 15, 121
Yungelson, L. R. 2008, AstL, 34, 620
Yungelson, L. R., Nelemans, G., & van den Heuvel, E. P. J. 2002, A&A, 388, 546
Zhao, J., & Heinke, C. O. 2023, MNRAS, Advance Access